

# Optimal control of a dissipative micromaser quantum battery in the ultrastrong coupling regime

Maristella Crotti,<sup>1,2</sup> Luca Razzoli,<sup>3,4</sup> Luigi Giannelli,<sup>5,6</sup> Giuseppe A. Falci,<sup>5,6</sup> and Giuliano Benenti<sup>1,2</sup>

<sup>1</sup>*Center for Nonlinear and Complex Systems, Dipartimento di Scienze e Alta Tecnologia, Università degli Studi dell'Insubria, Via Valleggio 11, 22100 Como, Italy*

<sup>2</sup>*INFN, Sezione di Milano, 20133 Milano, Italy*

<sup>3</sup>*Dipartimento di Fisica 'Alessandro Volta', Università di Pavia, Via Bassi 6, 27100 Pavia, Italy*

<sup>4</sup>*INFN, Sezione di Pavia, 27100 Pavia, Italy*

<sup>5</sup>*Dipartimento di Fisica e Astronomia 'Ettore Majorana', Università di Catania, Via S. Sofia 64, 95123 Catania, Italy*

<sup>6</sup>*INFN, Sezione di Catania, 95123 Catania, Italy*

(Dated: January 16, 2026)

We investigate the open system dynamics of a micromaser quantum battery operating in the ultrastrong coupling (USC) regime under environmental dissipation. The battery consists of a single-mode electromagnetic cavity sequentially interacting, via the Rabi Hamiltonian, with a stream of qubits acting as chargers. Dissipative effects arise from the weak coupling of the qubit–cavity system to a thermal bath. Non-negligible in the USC regime, the counter-rotating terms substantially improve the charging speed, but also lead, in the absence of dissipation, to unbounded energy growth and highly mixed cavity states. Dissipation during each qubit–cavity interaction mitigates these detrimental effects, yielding steady-state of finite energy and ergotropy. Optimal control on qubit preparation and interaction times enhances battery's performance in: (i) Maximizing the stored ergotropy through an optimized charging protocol; (ii) Stabilizing the stored ergotropy against dissipative losses through an optimized measurement-based passive-feedback strategy. Overall, our numerical results demonstrate that the interplay of ultrastrong light–matter coupling, controlled dissipation, and optimized control strategies enables micromaser quantum batteries to achieve both enhanced charging performance and long-term stability under realistic conditions.

## I. INTRODUCTION

Advances in quantum science and technology [1–4] have inspired investigations into energy storage at the quantum scale, leading to the concept of quantum batteries. Quantum batteries are quantum devices designed to store finite amounts of energy and release them upon request [5–7]. Their operation fundamentally relies on quantum effects: unitary charging processes can generate coherences between energy levels and, in many-body systems, entanglement between subsystems. These quantum features can enhance the performance of energy storage beyond what is achievable classically [8–14].

In realistic implementations [15–22], quantum batteries inevitably interact with their environment, causing effects such as dissipation and decoherence that can strongly affect their performance. To mitigate these effects, control strategies, first applied to closed-system settings [23–26], have been recently extended to the context of open quantum batteries [23–26].

Among the various models proposed for implementing a quantum battery, the micromaser architecture [27–29] plays a significant role, as it provides a physically realistic and widely studied setup. This system can be understood as a collision model [30], where a single-mode electromagnetic cavity acts as the energy-storage unit and is charged by a stream of two-level systems (atoms or other qubits) that interact sequentially with the cavity field [31–34].

In this paper, we focus on the micromaser operating in the ultrastrong coupling (USC) regime [35–45],

where the interaction strength is comparable to the system's natural frequencies and the light–matter interaction can no longer be treated perturbatively, giving rise to strongly correlated light–matter states and complex dynamics. Working in the USC regime is particularly relevant here because the enhanced light–matter interaction enables the micromaser quantum battery to charge significantly faster than in weaker coupling regimes.

We describe the dynamics of the open micromaser quantum battery using the formalism of open quantum systems [46–49], in which the battery and the chargers form the system of interest while the environment is modeled as a thermal bath of harmonic oscillators. Building on this framework, we investigate the time evolution of a micromaser quantum battery operating in the USC regime under realistic environmental interactions. We show that dissipation naturally stabilizes the battery, preventing unbounded energy growth. Moreover, we employ techniques from quantum optimal control [50] to design protocols that enhance the ergotropy, that is, the maximum amount of extractable work through unitary operations. Additionally, we propose a measurement-based passive feedback scheme to protect the stored ergotropy against dissipative losses.

Despite extensive studies on quantum batteries, the combined effects of USC and dissipation remain largely unexplored. Our work addresses this gap, providing insights into the interplay between strong light–matter interaction, environmental effects, and control strategies, thereby contributing to clarify the fundamental limits

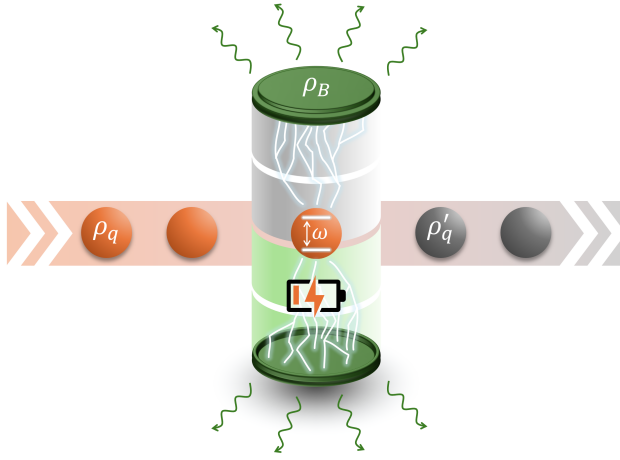


FIG. 1. Pictorial representation of the micromaser quantum battery. The battery, modeled as a single-mode cavity in the state  $\rho_B$ , interacts sequentially with a stream of identically prepared two-level systems (qubits)  $\rho_q$ . The qubits enter the cavity, exchange energy with the cavity field, and exit in the modified state  $\rho'_q$ . The wavy arrows indicate coupling to the environment, modeling dissipation of the cavity field. The sequential interactions, duration and qubit preparation, are designed to increase the amount of energy stored in the cavity field.

and opportunities of micromaser quantum batteries.

The paper is organized as follows. In section II, we introduce the model of the micromaser quantum battery, the Gorini-Kossakowski-Lindblad-Sudarshan (GKLS) master equation governing the open system dynamics, and the figures of merit by which we characterize the battery's performance. Then, after discussing the numerical results for both the non-dissipative and dissipative system dynamics, we elaborate on the optimal control strategies for the charging and stabilization protocols in section III. Finally, we present our main conclusions and outlooks in section IV.

## II. MODEL

### A. Micromaser quantum battery

The focus of our analysis is a specific and conceptually rich model of quantum battery based on the micromaser architecture. The micromaser battery consists of a single-mode electromagnetic field confined in a high-quality cavity, which serves as the quantum battery ( $B$ ), that sequentially interacts with a stream of identically prepared two-level quantum systems (atomic [51] or superconducting [39] qubits)  $\{q_k\}$  [31, 33] (see figure 1 for a pictorial representation). In the ideal model, the stream of qubits has fixed velocity and the rate of injection is low enough that the atoms traverse the cavity one by one (i.e., there are never two atoms in the cavity at the

same time). Moreover, under realistic conditions, qubits can be assumed to be non-interacting and initially uncorrelated with each other. Therefore, the dynamics is described by a basic Markovian collision model.

Each qubit interacts with the cavity for a fixed time interval  $\tau$ . The interaction between the qubit and the cavity mode is well-described by the quantum Rabi model [29, 52], whose total Hamiltonian is given by<sup>1</sup>

$$\hat{H}_{B,q} = \hat{H}_{B,q}^{(0)} + \hat{V}_{B,q}, \quad (1)$$

where the free and interaction Hamiltonians are, respectively,

$$\hat{H}_{B,q}^{(0)} \equiv \hat{H}_B + \hat{H}_q = \hbar\omega_B \hat{a}^\dagger \hat{a} + \hbar \frac{\omega_q}{2} \hat{\sigma}_z, \quad (2)$$

$$\hat{V}_{B,q} \equiv \hbar g (\hat{a} \hat{\sigma}_+ + \hat{a}^\dagger \hat{\sigma}_- + \hat{a}^\dagger \hat{\sigma}_+ + \hat{a} \hat{\sigma}_-). \quad (3)$$

Here,  $\hat{a}^{(\dagger)}$  is the cavity annihilation (creation) operator,  $\hat{\sigma}_{+(-)}$  is the qubit raising (lowering) operator,  $\hat{\sigma}_z$  is the Pauli  $z$  operator,  $\hbar$  is the reduced Planck constant (we set  $\hbar = 1$  throughout),  $\omega_{q(B)}$  is the qubit (cavity) frequency, and  $g$  is the coupling strength between the field and the qubit. We focus on the resonant case where the qubit and cavity frequencies are matched, i.e.,  $\omega_q = \omega_B \equiv \omega$ .

The coupling constant  $g$  measures the strength of the interaction between the qubits and the cavity. In cavity-QED implementations [51], when the coupling strength is much smaller than the bare frequencies ( $g \ll \omega_B, \omega_q$ ), the dynamics is accurately captured by the Jaynes-Cummings (JC) model. This model is obtained by applying the rotating-wave approximation (RWA), which allows us to neglect the so-called *counter-rotating terms*, the last two terms in the interaction Hamiltonian  $\hat{V}_{B,q}$ , that do not conserve the excitation number  $\hat{N} = \hat{a}^\dagger \hat{a} + \hat{\sigma}_+ \hat{\sigma}_-$  of the system. However, in circuit-QED [39] one can address the USC regime, where  $g$  becomes comparable to the cavity and qubit frequencies, the RWA breaks down, and the JC model is no longer valid [54]. Light and matter become strongly coupled, and the counter-rotating processes significantly modify the excitation-exchange mechanisms. These non-perturbative features have been shown to enhance charging speed and energy-storage capabilities in quantum batteries [31], which motivates our focus on the micromaser specifically operating in the USC regime.

<sup>1</sup> In what follows, we discuss the micromaser quantum battery in the Schrödinger picture, where the total Hamiltonian (1) is time-independent. This choice allows us to directly apply the GKLS master equation (10). In the interaction picture, instead, the presence of counter-rotating terms renders the Hamiltonian (1) explicitly time-dependent, thereby complicating both the derivation and the interpretation of the open system dynamics. We stress this point because previous works addressed the micromaser battery dynamics in the interaction picture [31, 33]. However, one should keep in mind that formulating a collision model in the interaction picture or in the Schrödinger picture generally corresponds to different physical scenarios, depending on the adopted representation [53].

Each qubit is initialized in a partially coherent state

$$\rho_q = q |g\rangle\langle g| + (1 - q) |e\rangle\langle e| + c\sqrt{q(1 - q)} (|e\rangle\langle g| + |g\rangle\langle e|), \quad (4)$$

where  $|g\rangle$  and  $|e\rangle$  denote the ground and excited states of the qubit, respectively. The parameter  $q \in [0, 1]$  controls the initial population inversion of the qubit, while the coherence parameter  $c \in [0, 1]$  determines the purity of the initial qubit state. The battery is initialized in its ground state, i.e.,  $\rho_B = |0\rangle\langle 0|$ .

During each interaction interval of duration  $\tau$ , the total system (cavity + qubit) evolves unitarily under the Hamiltonian  $\hat{H}_{B,q}$  (1). The state of the battery after each collision is obtained by tracing out the qubit

$$\rho_B(k) = \text{Tr}_q \left[ \hat{U}_{B,q}(\tau, 0) (\rho_B(k-1) \otimes \rho_q) \hat{U}_{B,q}^\dagger(\tau, 0) \right], \quad (5)$$

where  $\rho_B(k)$  is the battery state after the  $k$ th collision, and  $\hat{U}_{B,q}(t, t_0) = \exp[-i\hat{H}_{B,q}(t - t_0)]$  is the time evolution operator generated by the total Hamiltonian. This iterative evolution defines the overall dynamics of the micromaser battery.

After each collision, letting  $\hat{H}_B = \omega \hat{a}^\dagger \hat{a}$  be the battery Hamiltonian, we monitor three relevant figures of merit, that serve as indicators of the battery's performance and coherence throughout the charging protocol: (i) the energy stored into the cavity (measured from the ground state),  $E(k) = \text{Tr}[\hat{H}_B \rho_B(k)]$ ; (ii) the purity of the cavity state,  $\mathcal{P}(k) = \text{Tr}[(\rho_B(k))^2]$ , which we use as an indicator of the degradation of the battery state; and (iii) the *ergotropy*  $\mathcal{E}(k)$  stored into the cavity, which quantifies the maximum amount of work extractable from the battery state  $\rho_B(k)$  with respect to the Hamiltonian  $\hat{H}_B$  via unitary transformations.

For a quantum system with Hamiltonian  $\hat{H} = \sum_k \epsilon_k |\epsilon_k\rangle\langle\epsilon_k|$  with  $\epsilon_{k+1} \geq \epsilon_k$  prepared in a state  $\rho = \sum_k r_k |r_k\rangle\langle r_k|$  with  $r_{k+1} \leq r_k$ , the ergotropy is defined as [55, 56]

$$\mathcal{E}(\rho) \equiv \text{Tr}[\hat{H}\rho] - \min_{\hat{U}} \text{Tr}[\hat{H}\hat{U}\rho\hat{U}^\dagger], \quad (6)$$

where the minimization is performed over all unitary operators  $\hat{U}$ . Solution of the minimization problem is the unitary  $\hat{U}_{\mathcal{E}} = \sum_k |\epsilon_k\rangle\langle r_k|$ , which maps the initial state  $\rho$  into  $\pi_{\mathcal{E}} \equiv \hat{U}_{\mathcal{E}}\rho\hat{U}_{\mathcal{E}}^\dagger = \sum_k r_k |\epsilon_k\rangle\langle\epsilon_k|$ . The state  $\pi_{\mathcal{E}}$  is referred to as *passive*, as it represents a quantum state from which no work can be extracted through unitary operations. In general, it can be shown that a state is passive if and only if it is diagonal in the energy eigenbasis  $\{|\epsilon_k\rangle\}$  and its eigenvalues decrease monotonically with energy (i.e., there is no population inversion) [57, 58],

$$\pi = \sum_k p_k |\epsilon_k\rangle\langle\epsilon_k|, \quad p_{k+1} \leq p_k. \quad (7)$$

Notably, provided the Hamiltonian  $\hat{H}$  has a non-

degenerate spectrum,<sup>2</sup> for any state  $\rho$  there exists a unique passive state  $\pi_{\mathcal{E}}$ , and the ergotropy can be expressed in terms of such state  $\mathcal{E}(\rho) = \text{Tr}[\hat{H}\rho] - \text{Tr}[\hat{H}\pi_{\mathcal{E}}]$ . According to equation (7), thermal (Gibbs) states  $G_{\beta} = \exp[-\beta\hat{H}]/\text{Tr}\{\exp[-\beta\hat{H}]\}$ —with  $\beta = 1/(k_B T)$  the inverse temperature—are passive, since they commute with  $\hat{H}$  and their eigenvalues do not increase with energy. Throughout, we set the Boltzmann constant  $k_B = 1$ .

## B. Dissipation

So far, we have described an ideal model, treating the micromaser battery as a closed quantum system. In practice, however, the system is never completely isolated from its environment. Interactions with the surroundings introduce dissipation and decoherence, which can strongly affect the system's dynamics.

To account for these effects, we describe the battery using the open-quantum-system framework. We model dissipation occurring during each qubit–cavity interaction, rather than only during idle periods between collisions as in previous studies [33]. To compensate for energy loss due to dissipation, qubits are injected in immediate succession, keeping the cavity continuously engaged in the charging process. This assumption leads to a more realistic model of the micromaser battery, as it accounts for the fact that the environment remains present and active even during the charging process. As a result, the dissipative dynamics should act on the full system composed of the cavity and the interacting qubit, which we denote collectively as  $S$ .

We model the environment as a thermal bath of harmonic oscillators in thermal equilibrium at inverse temperature  $\beta$ , with Hamiltonian

$$\hat{H}_E = \sum_k \omega_k \hat{b}_k^\dagger \hat{b}_k, \quad (8)$$

where  $\hat{b}_k$  and  $\hat{b}_k^\dagger$  are the annihilation and creation operators for the  $k$ th bath mode of frequency  $\omega_k$ . The system–bath interaction is described by a coupling of the form

$$\hat{H}_I = \hat{V} \otimes \sum_k g_k (\hat{b}_k^\dagger + \hat{b}_k), \quad (9)$$

where  $\hat{V}$  is the system operator through which  $S$  couples to the bath, and  $g_k$  are coupling constants.

Following the standard theory of open quantum systems [46–49], the evolution of the joint system state  $\rho_S(t)$

<sup>2</sup> If the Hamiltonian spectrum is degenerate, the passive state is defined up to unitaries acting in each degenerate subspace.

is governed by a GKLS master equation [59–61]

$$\begin{aligned} \frac{d}{dt}\rho_S(t) &= -i[\hat{H}_S, \rho_S(t)] \\ &+ \sum_{\omega} \left( \hat{L}_{\omega}\rho_S(t)\hat{L}_{\omega}^{\dagger} - \frac{1}{2} \left\{ \hat{L}_{\omega}^{\dagger}\hat{L}_{\omega}, \rho_S(t) \right\} \right), \end{aligned} \quad (10)$$

where  $\hat{H}_S = \sum_{\epsilon} \epsilon |\epsilon\rangle\langle\epsilon|$  is the total Hamiltonian of the qubit–cavity system during the collision (see equation (1)),  $[\cdot, \cdot]$  denotes the commutator, and  $\{\cdot, \cdot\}$  the anti-commutator. Here, the sum runs over the Bohr frequencies  $\omega = \epsilon' - \epsilon$ , which correspond to energy differences between eigenstates  $|\epsilon'\rangle$  and  $|\epsilon\rangle$  of  $\hat{H}_S$ . These frequencies determine the allowed transitions through which the system can exchange energy with the environment.

The Lindblad operators  $\hat{L}_{\omega}$  describe energy exchanges between the system and the environment, and are defined as

$$\hat{L}_{\omega} = \sqrt{\gamma(\omega)} \sum_{\epsilon' - \epsilon = \omega} V_{\epsilon\epsilon'} |\epsilon\rangle\langle\epsilon'|, \quad (11)$$

where  $V_{\epsilon\epsilon'} = \langle\epsilon|\hat{V}|\epsilon'\rangle$ . Although the dissipation acts on the full system  $S$ , we assume that only the cavity is directly coupled to the environment. Accordingly, we take the system operator  $\hat{V}$  to be

$$\hat{V} = (\hat{a} + \hat{a}^{\dagger}) \otimes \mathbb{I}_q, \quad (12)$$

where  $\mathbb{I}_q$  is the identity on the qubit subspace. This reflects the physical picture in which the cavity is a fixed, central component of the micromaser battery, permanently present and exposed to the environment, whereas the qubits are transient ancillae injected one at a time.

The decay rate associated with a transition at Bohr frequency  $\omega$  is given by [62, 63]

$$\gamma(\omega) = \frac{2\pi J(|\omega|)}{1 - e^{-\beta|\omega|}} \left( \Theta(\omega) + e^{-\beta|\omega|} \Theta(-\omega) \right), \quad (13)$$

where  $\Theta(\omega)$  is the Heaviside step function and  $J(\omega)$  is the spectral density of the environment. The two contributions describe spontaneous and stimulated emission ( $\omega > 0$ ) and absorption ( $\omega < 0$ ) processes, respectively.

We assume an Ohmic spectral density with exponential cutoff,

$$J(\omega) = \eta |\omega| e^{-|\omega|/\omega_c}, \quad (14)$$

where  $\eta$  is a coupling constant and  $\omega_c$  is a cutoff frequency characterizing the bath's correlation timescale.

### III. NUMERICAL RESULTS

We present here the results of the numerical investigation of the micromaser quantum battery dynamics. We begin by exploring the closed-system dynamics of the battery in the absence of dissipation, then turn to

the open-system case to investigate how environmental effects influence the dynamics, and finally consider parameter optimization for both the charging and stabilization processes. All simulations are carried out using the open-source QuTiP library for Python [64, 65], while the optimization of system parameters is performed with the `minimize` routine from `scipy.optimize`, employing the Broyden-Fletcher-Goldfarb-Shanno (BFGS) quasi-Newton method [66] to efficiently explore the parameter landscape.

#### A. Non-dissipative dynamics

We start our study by numerically investigating the charging dynamics of the micromaser quantum battery in the non-dissipative regime, where each qubit–cavity collision is treated as a unitary evolution (closed system dynamics). Although the battery's reduced dynamics are open due to repeated interactions, we refer to this as a closed quantum battery, as there is no coupling to an external environment. Figure 2 shows the energy, purity, and ergotropy as functions of the number of collisions, for four values of the coupling strength  $g$  in the USC regime. Both the cavity energy and ergotropy increase indefinitely with the number of collisions, showing no sign of stabilization, while the purity rapidly decreases, indicating that the battery evolves into strongly mixed states. These effects are more pronounced at larger coupling strengths, with faster growth of energy and ergotropy and a more rapid decrease of purity, reflecting the stronger energy transfer and enhanced mixing induced by the counter-rotating terms in the Rabi Hamiltonian (1). Our simulations also confirm that variations in the qubit preparation have only a modest influence on this behavior: coherence plays a minor role, while population inversion mainly affects the charging rate.

Overall, in the absence of dissipation, the counter-rotating terms lead to unbounded energy growth and increasingly mixed cavity states, which makes it challenging to control and exploit the energy stored in the cavity.

#### B. Dissipative dynamics

We then turn to the numerical study of the dissipative dynamics of the micromaser quantum battery, where each qubit–cavity collision is treated as the evolution of an open quantum system due to the coupling to an external environment. We therefore refer to this as an open quantum battery. Including dissipation during each qubit–cavity collision qualitatively changes the dynamics in the USC regime. As shown in figure 3, energy and ergotropy, which grew unboundedly in the closed system, now converge to well-defined steady-state values. Purity is also higher than in the non-dissipative case, particularly at small coupling, and decreases moderately with

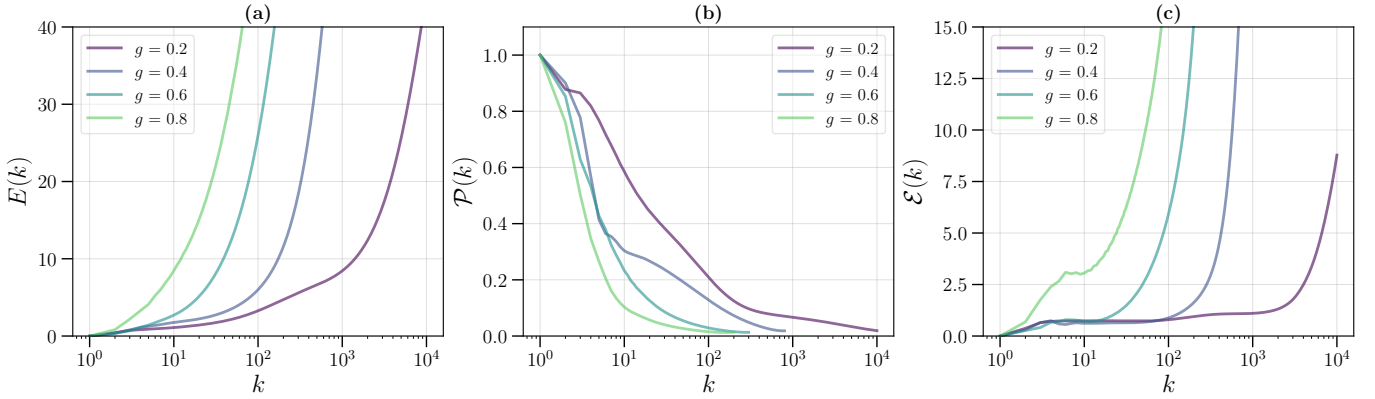


FIG. 2. Evolution of the closed quantum battery: (a) energy, (b) purity, and (c) ergotropy as functions of the number of collisions. Each curve corresponds to a different coupling strength in the USC regime,  $g \in \{0.2, 0.4, 0.6, 0.8\}$ , with fixed parameters  $c = 1$ ,  $q = 0.5$ ,  $\tau = 10$ , and  $\omega = 1$ . In the closed-system regime, both the cavity energy and ergotropy increase without bound as the number of collisions grows, while the purity rapidly decreases, indicating that the battery evolves into strongly mixed states.

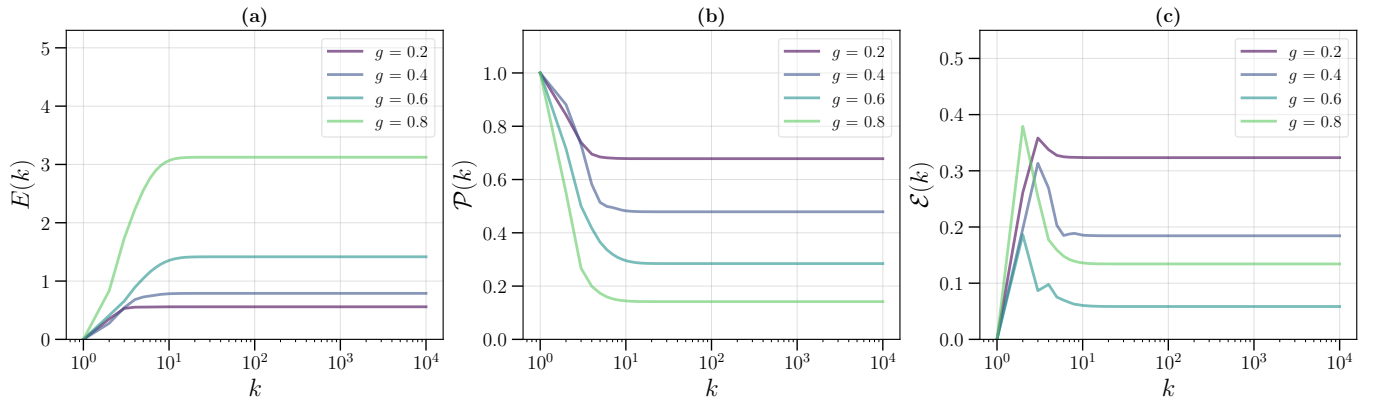


FIG. 3. Evolution of the open quantum battery: (a) energy, (b) purity, and (c) ergotropy as functions of the number of collisions. Each line corresponds to a different value of  $g \in \{0.2, 0.4, 0.6, 0.8\}$  in the USC regime, with fixed system parameters  $c = 1$ ,  $q = 0.5$ ,  $\tau = 10$ ,  $\omega = 1$ , and environment parameters  $\omega_c = 3$ ,  $\beta = 450$ , and  $\eta = 0.01$ . Including dissipation during each qubit–cavity collision qualitatively changes the dynamics: energy and ergotropy converge to well-defined steady-state values, while purity decreases moderately with increasing  $g$ . The steady-state ergotropy remains nonzero, indicating that the energy stored in the cavity is at least partially extractable through unitary operations.

increasing  $g$ . Importantly, the steady-state ergotropy is nonzero, indicating that the energy stored in the cavity remains at least partially extractable through unitary operations. These results demonstrate that environmental dissipation provides a stabilizing mechanism, suppressing the instabilities induced by counter-rotating terms and allowing the micromaser battery to store finite, extractable energy.

In our analysis of the open system dynamics of the micromaser battery, we use environmental parameters  $\eta = 0.01$ ,  $\beta = 450$ , and  $\omega_c = 3$ , corresponding to a dimensionless single-photon loss rate of  $\gamma/\omega \simeq 0.045$ , which yields a decay time of  $T_1 \approx 22$  (in units of  $\omega^{-1}$ ). In contrast, typical cavity decay rates reported for experimental setups operating in the USC regime, such as those in circuit QED [38, 67–69], are of the order of  $10^{-4}$  (in units of the cavity frequency), i.e., about two

orders of magnitude lower than the effective loss rate used in our simulations. The reason for employing comparatively large dissipation values, while still remaining within the weak system-environment coupling regime required by the GKLS formalism, is primarily computational. Numerically implementing the single-mode field of the cavity requires a truncated Fock basis with a sufficient number of excited states: the larger the Hilbert space, the more accurate the simulation, the higher the computational cost. In practice, one restricts the Fock basis to the minimum number of excited states such that the highest ones are not effectively involved in the dynamics. When a continuous stream of qubits interacts with the cavity, low dissipation typically allows highly excited states to become significantly populated during the charging process, saturating the truncated Fock basis, and thus compromising the reliability of the numer-

ical simulation. Stronger dissipation, instead, allows us to keep the cavity population well within the numerically accessible subspace, while still retaining meaningful physical behavior. Therefore, our simulations, which already reveal promising results for both ergotropy and stored energy, suggest that the performance of the micromaser battery would likely be further enhanced under realistically weaker dissipation.

### C. Optimal control

The results obtained so far motivate the next step of our analysis: designing optimized charging and stabilization protocols for the dissipative micromaser quantum battery. Our study focuses on maximizing the ergotropy stored in the battery within a finite number of collisions with the qubit stream and on maintaining this ergotropy against dissipation once the battery is charged.

Optimal control theory provides a systematic framework to achieve these goals, by tuning control parameters such as the qubit population inversion and the interaction times with the cavity to optimize a well-defined cost function. In the context of quantum batteries [18, 70], this enables the design of charging and storage protocols that enhance the battery’s performance, even in the presence of dissipation and non-ideal effects.

#### 1. Charging process

Our goal is to design an optimal charging protocol for the micromaser quantum battery that maximizes the stored ergotropy, under the constraint of a limited amount of resources, i.e., a finite stream of qubits. We optimize over two sets of control parameters: the initial population inversion of the qubit,  $q$  (see equation (4)), which is taken to be the same for all collisions, and the interaction times,  $\{\tau_k\}$ , that are allowed to vary from collision to collision. The optimization problem—i.e., maximizing the final ergotropy of the system,  $\mathcal{E}_F$ —is reformulated as the minimization of a *cost function* defined as  $\mathcal{C} = -\mathcal{E}_F$ .

We consider a setting close to realistic experimental conditions, where the total number of collisions between the qubits (chargers) and the cavity (battery) is fixed in advance due to practical constraints, and the charging protocol is optimized under this constraint. This choice is justified by the fact that, for the dissipation parameters used (the same as in figure 3), the system reaches its steady state after only a small number of collisions ( $N_{\text{col}} \simeq 10$ ). It is therefore natural to focus on the first collisions, which are the most relevant for maximizing the stored ergotropy. For this reason, in our simulations we fix the number of collisions to  $N_{\text{col}} = 5$ .

We set the physical parameters of the model as follows:

$c = 1$ <sup>3</sup> and  $\omega = 1$  for the system, and  $\eta = 0.01$ ,  $\omega_c = 3$ ,  $\beta = 450$  for the environment, as in section III B. While keeping these parameters fixed, we scanned values of the coupling constant  $g \in [0.1, 0.7]$ , ranging from weaker to stronger coupling strengths while remaining in the USC regime.

Optimization problems often suffer from local minima of the cost function, which result in sub-optimal solutions. To increase confidence that the obtained minimum of  $\mathcal{C}$  corresponds to a *global* minimum, rather than a local one, we performed multiple optimizations starting from different initial conditions for the parameters to be optimized, randomly sampled within preset boundaries. This approach allows us to explore different regions of the parameter space of  $q$  and  $\{\tau_k\}$ , thereby increasing the likelihood that the resulting configuration indeed maximizes the final ergotropy  $\mathcal{E}_F$ .

To assess the effectiveness of our optimized protocol, we compare our results with a natural benchmark choice of collision times, given by

$$\tau_k = \frac{\pi}{2g\sqrt{k}}, \quad k = 1, \dots, N_{\text{col}}, \quad (15)$$

while fixing  $q = 0$ , that is, the qubit is prepared in its excited state. This choice is motivated by the JC model, where, at resonance, the interaction between a two-level system and a quantized field mode produces Rabi oscillations with frequency  $\Omega_n = 2g\sqrt{n}$ . Setting the interaction time to  $\tau(n) = \pi/(2g\sqrt{n})$  implements a  $\pi$ -pulse on the transition  $|e, n-1\rangle \leftrightarrow |g, n\rangle$ , thereby making the qubit and the cavity exchange a single excitation. In practice, if the cavity starts in the Fock state  $|n-1\rangle$  and the qubit in  $|e\rangle$ , after an interaction time  $\tau(n)$  the joint state evolves to  $|g, n\rangle$ : the qubit relaxes to the ground state and the cavity gains one photon. Therefore, the optimal charging protocol in the ideal JC model requires  $q = 0$  and  $\tau(n)$ , as this procedure maximizes the energy transfer at each collision, with the cavity effectively charging by one photon per interaction. This prescription, which we refer to as the  $\pi$ -pulse protocol in the following, provides a natural benchmark against which we can compare the performance of our optimized protocol, even though the dynamics of our micromaser model is governed by the full Rabi Hamiltonian (1), which, unlike the JC Hamiltonian, does not preserve the total number of excitations, and is subject to dissipation.

Figure 4(a) shows the ergotropy of the optimized protocol as a function of the number of collisions  $k$ , for the cases  $g \in \{0.1, 0.7\}$ . The results confirm that the optimization is indeed highly effective: for both values of  $g$ , the optimized protocol achieves significantly higher ergotropy compared with the  $\pi$ -pulse protocol ( $q = 0$  and

<sup>3</sup> Initially, we also optimized the parameter  $c$ ; however, we observed that most optimizations yielded  $c = 1$  as the optimum. Therefore, to improve computational efficiency, we fixed  $c = 1$  and excluded it from further optimization.

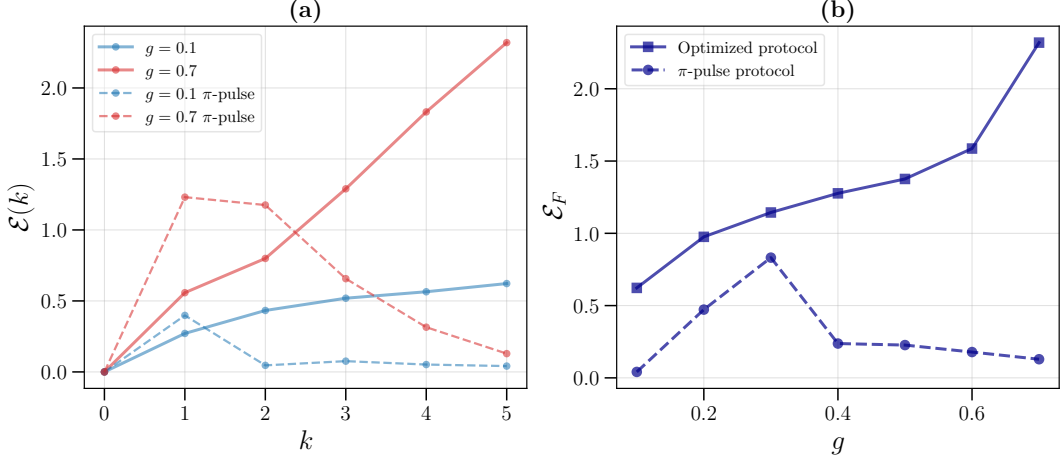


FIG. 4. Comparison of ergotropy in optimized and non-optimized protocols. (a) Optimized battery ergotropy as a function of the number of collisions (solid curves), compared with the non-optimized one resulting from the  $\pi$ -pulse protocol (dashed curves) defined by the Jaynes-Cummings prescription  $\tau_k = \pi/(2g\sqrt{k})$  with  $q = 0$ . Blue curves correspond to  $g = 0.1$ , while red curves correspond to  $g = 0.7$ . The optimized protocol consistently achieves higher final ergotropy than the  $\pi$ -pulse protocol, demonstrating the effectiveness of the optimization. (b) Battery final ergotropy as a function of the coupling constant  $g$ , comparing optimized protocols (solid line) with  $\pi$ -pulse protocols (dashed line). Across all values of  $g$ , the optimized protocols consistently yield higher final ergotropy. Fixed parameters:  $c = 1$ ,  $\omega = 1$ ,  $\omega_c = 3$ ,  $\eta = 0.01$ , and  $\beta = 450$ .

$\tau_k$  (15)). At intermediate collisions, the ergotropy in the  $\pi$ -pulse protocol (dashed lines) can temporarily exceed that in the optimized protocol (solid lines). This behavior arises because the optimization is designed to maximize the *final* ergotropy rather than the ergotropy at each intermediate collision. Overall, jointly optimizing the interaction times and the qubit preparation significantly increases the ergotropy, demonstrating that proper tailoring of the charging protocol can enhance performance.

Figure 4(b) shows the final ergotropy of the optimized protocols compared with the  $\pi$ -pulse protocol, as a function of  $g$ . This plot summarizes the overall performance of the micromaser battery, demonstrating that the optimized protocols consistently achieve higher final ergotropy than the non-optimized one. In addition, the final ergotropy grows with increasing  $g$ , reflecting the enhanced energy transfer at stronger coupling strengths.

To further illustrate the effectiveness of the optimized protocol, we analyze the Wigner quasi-probability distribution of the battery state after the charging process. Unlike classical probability distributions, it can take negative values, reflecting the intrinsically quantum nature of the state. In addition to capturing the state's phase-space structure, the Wigner function also encodes information about its energy, as expectation values of observables, including the Hamiltonian, can be computed as integrals over phase space weighted by the Wigner function [71, 72]. Figure 5 shows the Wigner functions for three cases: the closed-system  $\pi$ -pulse protocol (figure 5(a)), the open-system  $\pi$ -pulse protocol (figure 5(b)), and the optimized open-system protocol (figure 5(c)), all corresponding to the parameters used for  $g = 0.7$  in figure 4(a). In the first case, the Wigner function exhibits some

negativities, whereas in the other two cases the distributions remain strictly non-negative, likely due to the dissipative nature of the open-system evolution, which tends to suppress quantum features that would otherwise produce negative regions. Qualitative differences are clearly visible: the non-optimized protocols, i.e., both the closed-system and open-system  $\pi$ -pulse protocols shown in panels (a) and (b), display an irregular, low-amplitude distribution near the origin, indicative of a moderately excited state. In contrast, the optimized protocol in panel (c) produces a distribution with larger amplitudes displaced away from the origin, signaling a higher energy content. This directly demonstrates that the optimization substantially enhances the charging performance.

## 2. Stabilization

Charging a battery is only the first step in its operation; the second is stabilizing the injected energy against losses. After optimizing the charging process, we now turn to the problem of stabilizing the ergotropy stored at the end of the charging stage. Our goal is to identify a strategy that maintains the ergotropy of the battery approximately constant over a prescribed time interval. Indeed, if the stream of qubits is simply switched off and the cavity is allowed to evolve freely, dissipation inevitably causes a progressive loss of energy and, consequently, of ergotropy. A dedicated stabilization protocol is therefore required to preserve the stored useful work against environmental degradation.

As a first approach, we simply leveraged the drive represented by the stream of qubits which sequentially

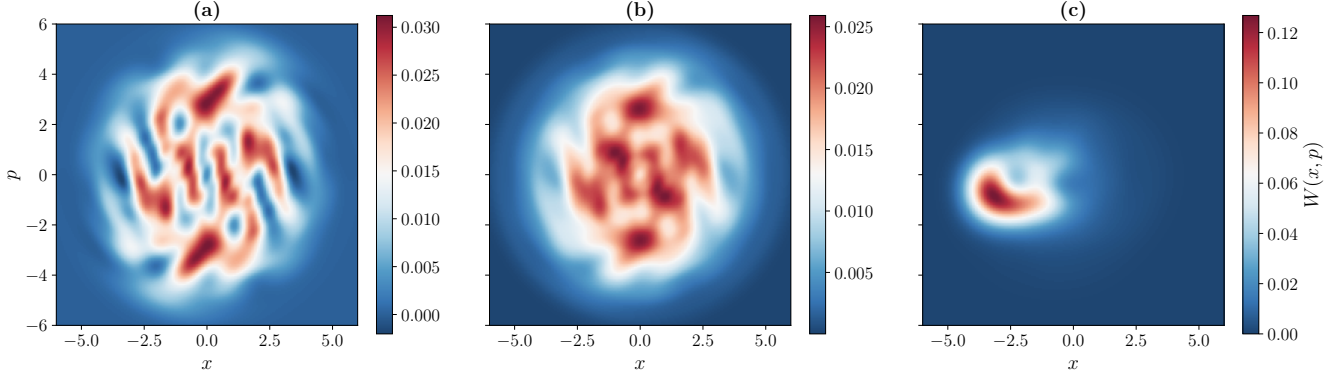


FIG. 5. Wigner function of the battery state after the charging process for three different protocols. (a) Closed-system  $\pi$ -pulse protocol with  $g = 0.7$ ,  $\tau_k = \pi/(2g\sqrt{k})$ ,  $q = 0$ ,  $c = 1$ , and  $\omega = 1$ . (b) Open-system  $\pi$ -pulse protocol with the same system parameters and environmental parameters  $\omega_c = 3$ ,  $\beta = 450$ , and  $\eta = 0.01$ . (c) Optimized open-system protocol, corresponding to the optimal parameters used for  $g = 0.7$  in figure 4(a). Panel (a) exhibits small negativities typical of quantum coherence, while panels (b) and (c) show strictly non-negative distributions due to dissipative effects. Panels (a) and (b) display irregular, low-amplitude distributions near the origin, indicative of moderately excited battery states, whereas panel (c) shows a distribution with larger amplitudes displaced away from the origin, signaling a higher energy content and enhanced charging performance.

interact with the cavity as a mechanism to counteract dissipation. Even upon optimizing over the parameters  $(q, \{\tau_k\})$ , this approach fails to stabilize the ergotropy, as no optimal parameters can be identified that preserve the stored ergotropy. Instead, the ergotropy decays even faster than if the cavity were left to evolve under dissipation alone, as shown in figure 6. This behavior arises because the continued interaction with the qubits progressively degrades the purity of the battery.

To improve this scheme, we devised a different strategy, in which each qubit is measured after its collision with the cavity. We refer to this mechanism as *passive feedback* because the measurement outcomes are not used to actively modify subsequent controls; rather, the measurement backaction itself alters the cavity state, counteracting dissipation and keeping the ergotropy accumulated during the charging stage approximately constant throughout the stabilization interval. To identify the most effective stabilization strategy, we adjusted the same control parameters optimized for the charging process, the qubit population  $q$  and the interaction times  $\{\tau_k\}$ , but with a different objective: rather than maximizing the growth of ergotropy, we now aim to minimize its deviation from the post-charging value, thereby keeping the stored ergotropy approximately constant.

To implement this, we simulated the dynamics using a measurement-based collision model, in which a projective measurement of energy is performed on each qubit after the collision, yielding two possible outcomes,  $\{|g\rangle, |e\rangle\}$ , corresponding to eigenvalues  $\mp\omega/2$ , respectively. Each possible sequence of outcomes defines a quantum trajectory  $\gamma$ , with an associated probability  $p_\gamma$ . For a given set of parameters  $(q, \{\tau_k\})$ , we compute the weighted average

ergotropy after each collision,

$$\bar{\mathcal{E}}(k) = \sum_{\gamma} p_{\gamma} \mathcal{E}_{\gamma}(k), \quad (16)$$

where  $\mathcal{E}_{\gamma}(k)$  is the ergotropy along the trajectory  $\gamma$  after the  $k$ th collision.

We then define a cost function that quantifies the deviation of the stored ergotropy from its initial value  $\mathcal{E}_{\text{in}}$  at the beginning of the stabilization stage,

$$\mathcal{C}(q, \{\tau_k\}) = \sum_{k=0}^N [\bar{\mathcal{E}}(k) - \mathcal{E}_{\text{in}}]^2, \quad (17)$$

where we fixed  $N = 10$ . Minimizing  $\mathcal{C}$  identifies the parameters that best preserve the stored ergotropy over the course of the stabilization protocol.

Figure 6 illustrates the charging and stabilization processes of the quantum battery. For the stabilization stage, we compare three scenarios: the passive-feedback protocol with optimized parameters, the continuous injection of qubits without measurement using the values of  $q$  and  $\{\tau_k\}$  obtained from the optimization of the stabilization protocol, and the evolution under dissipation alone. The fixed parameters used in the simulations are  $g = 0.7$ ,  $c = 1$ ,  $\omega = 1$ ,  $\eta = 0.01$ ,  $\omega_c = 3$ , and  $\beta = 450$ . Thus, the charging process corresponds to the optimized protocol with  $g = 0.7$  shown in figure 4(a). The results show that the passive-feedback protocol, combined with optimized control parameters, effectively stabilizes the battery. In contrast, free evolution under dissipation leads to a gradual decay of ergotropy, while injecting qubits without measurement performs even worse for

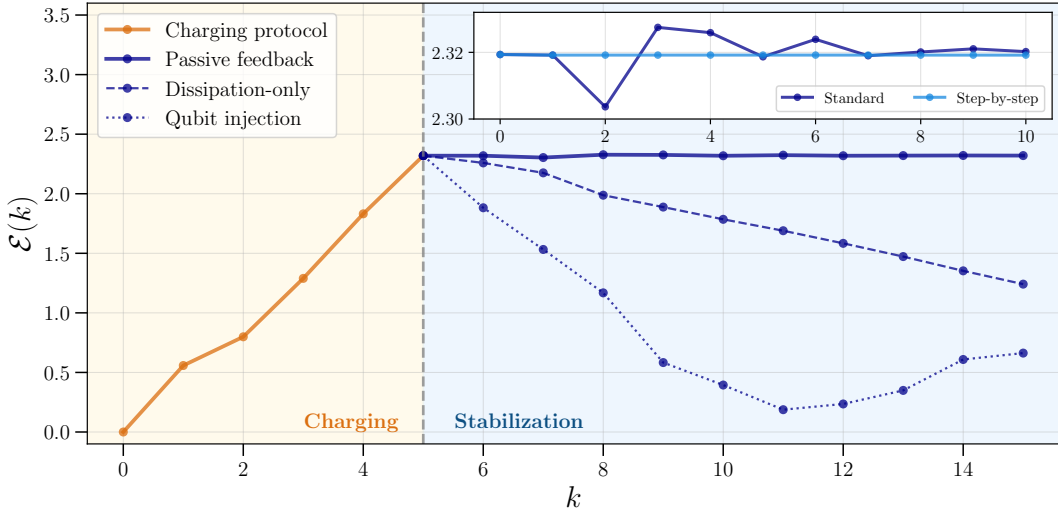


FIG. 6. Charging and stabilization of the open quantum battery. The charging protocol corresponds to the optimized process with  $g = 0.7$  shown in figure 4(a). The stabilization stage is compared across three scenarios: the passive-feedback protocol with optimized parameters, the continued injection of qubits without measurement using the same  $q$  and  $\{\tau_k\}$  as in the optimized stabilization protocol, and the evolution under dissipation alone. Parameters are fixed at  $g = 0.7$ ,  $c = 1$ ,  $\omega = 1$ ,  $\eta = 0.01$ ,  $\omega_c = 3$ , and  $\beta = 450$ . The passive-feedback protocol successfully maintains the stored ergotropy, while dissipation alone causes gradual decay and qubit injection without measurement leads to a rapid drop in ergotropy after only 10 collisions. The inset shows the optimized passive-feedback stabilization protocol obtained from two different procedures: the standard optimization reported in the main figure and a step-by-step approach in which the interaction times  $\{\tau_k\}$  are sequentially adjusted to stabilize the ergotropy after each collision, while keeping  $q$  fixed at the value obtained from the standard optimization. The step-by-step procedure yields a smoother and more stable ergotropy profile with reduced fluctuations compared to the standard protocol.

the parameters considered, causing a significant drop in ergotropy after only 10 collisions.

In the inset of figure 6, we compare the performance of the passive-feedback stabilization protocol under two different optimizations: the standard approach described above (the cost function (17) is minimized over the whole trajectory), and a step-by-step approach, in which stabilization is enforced at each collision (the cost function  $\mathcal{C}(\tau_k) = [\bar{\mathcal{E}}(k) - \mathcal{E}_{\text{in}}]^2$  is minimized at each collision). In the latter approach, the interaction times  $\{\tau_k\}$  are optimized sequentially after each collision, while keeping  $q$  fixed at the value obtained from the standard optimization, so as to maintain the ergotropy approximately constant throughout the evolution. This procedure results in a smoother ergotropy profile with reduced fluctuations compared to the standard protocol.

We point out that, while step-by-step optimization is meaningful in the stabilization protocol, it is not suitable in the charging protocol, where the goal is to maximize the *final* ergotropy  $\mathcal{E}_F$ . Step-by-step optimization is a “greedy” strategy that locally optimizes each collision, and a trajectory through locally optimal solutions may fail to reach the global optimum. In our setting, step-by-step maximization of the ergotropy  $\mathcal{E}(k)$  at each collision does not reproduce the globally optimized protocol for  $\mathcal{E}_F$ , typically resulting in lower final ergotropy and worse overall performance. In contrast, in the stabilization protocol the objective is to maintain a nearly con-

stant ergotropy throughout the evolution,  $\bar{\mathcal{E}}(k) \approx \mathcal{E}_{\text{in}}$ . In this case, a step-by-step optimization, in which ergotropy fluctuations are minimized at each collision, is more appropriate and numerically accurate than a global optimization, in which ergotropy fluctuations are minimized over the entire trajectory. Indeed, we have numerically identified a stabilization protocol that maintains constant ergotropy (see inset of figure 6). Although this protocol is, in principle, a solution of both the global and the step-by-step optimization, the latter optimization proves more effective in practice at identifying it, thereby achieving a more accurate stabilization of the stored ergotropy.

#### IV. CONCLUSION

We have investigated a dissipative micromaser quantum battery operating in the ultrastrong coupling (USC) regime, with a focus on the optimization of the charging protocol and the stabilization of the stored ergotropy against losses. Building on the framework of collision models, the battery, modeled as a single-mode electromagnetic cavity, repeatedly interacts with a stream of two-level systems (qubits) acting as chargers. Each interaction is governed by the Rabi Hamiltonian, as counter-rotating terms cannot be neglected in the USC regime. Under the assumption of a weak coupling between the system of interest (battery and chargers) and an exter-

nal Markovian environment, we have numerically investigated the dissipative dynamics of the micromaser battery through a GKLS master equation, and characterized its performance in terms of stored energy, purity of the battery state, and stored ergotropy. Besides ensuring a more realistic modelling, dissipation plays a beneficial role by effectively stabilizing the charging process. It prevents the unbounded growth of the energy stored in the cavity and drives the battery towards steady states with finite ergotropy and higher purity compared to the non-dissipative dynamics. This reveals the capability of the micromaser battery to store useful energy even in the presence of environmental losses. Our results show that stronger light-matter couplings in the USC regime lead to faster battery charging and greater stored energy and ergotropy.

We optimized the battery's charging protocol by leveraging collision-dependent interaction times  $\{\tau_k\}$  and the qubit population parameter  $q$ , aiming to maximize the final ergotropy within a finite number of collisions, i.e., with limited number of chargers. Numerical routines were employed to explore the control landscape, and multiple runs from different initial guesses increased the likelihood of locating global optima. Our analysis shows that such optimization significantly enhances battery's performance: after only a few collisions, the ergotropy stored under the optimal protocol is consistently higher than that in benchmark strategies, such as the  $\pi$ -pulse protocol representing the optimal energy-transfer strategy in the weak-coupling limit (Jaynes-Cummings model).

After the charging stage, to stabilize the ergotropy stored in the battery we propose a measurement-based passive-feedback protocol, in which each charger qubit is measured after interacting with the cavity. Upon optimizing the control parameters  $q$  and  $\{\tau_k\}$  to minimize deviations of the ergotropy from its post-charging value, this mechanism effectively counteracts dissipative losses and maintains the stored ergotropy approximately constant over a desired time interval. This passive-feedback protocol remarkably outperforms all other strategies we considered, including using the stream of qubits as a drive without measurements, a strategy which can perform even worse than letting the cavity evolve freely under dissipation.

It is worth emphasizing that our open-system simulations rely on conservative assumptions for dissipation, with a dimensionless single-photon loss rate  $\gamma/\omega \simeq 0.045$  (see Sec. III B). This value exceeds by approximately two orders of magnitude the typical cavity decay rates  $\gamma/\omega \sim 10^{-4}$  reported in circuit-QED experiments in the USC regime [38, 67–69]. As a consequence, our results are likely to underestimate the achievable performance in

realistic experimental platforms.

In conclusion, our work reveals the rich interplay between strong light-matter interaction, environmental effects, and optimal-control strategies in determining the performance of quantum batteries, underscoring the potentially beneficial role of dissipation. Specifically, we have shown that a dissipative micromaser quantum battery operating in the USC regime can be effectively stabilized and its performance significantly enhanced through optimal control techniques. This paves the way for a systematic design of quantum energy-storage devices in which dissipation and control are complementary resources to leverage to improve the operational robustness. Several promising directions for future work can be envisaged. One possibility is to explore multiobjective optimizations, e.g., aiming to enhance the tradeoff between charging power and stored ergotropy. Another is to investigate the role of non-Markovianity by considering collision models with initially correlated or pairwise interacting charger qubits, and to explore the simultaneous injection of multiple qubits into the cavity. Finally, incorporating continuous monitoring of the environment [73–81] or actively engineering the bath itself could open further possibilities for control and work extraction.

## ACKNOWLEDGMENTS

G.B. acknowledges useful discussions with Dario Ferraro. M.C. and G.B. acknowledge support from INFN through the project “QUANTUM” and from the European Union-NextGenerationEU through the “Solid State Quantum Batteries: Characterization and Optimization” (SoS-QuBa) project (Prot. 2022XK5CPX), in the framework of the PRIN 2022 initiative of the Italian Ministry of University (MUR) for the National Research Program (PNR). This project has been funded within the programme “PNRR Missione 4- Componente 2 Investimento 1.1 Fondo per il Programma Nazionale di Ricerca e Progetti di Rilevante Interesse Nazionale (PRIN)”, funded by the European Union-Next Generation EU. L.R. acknowledges support from University of Pavia through the project “Termodinamica di precisione per sistemi aperti quantistici”, funded within the “Fondo Ricerca e Giovani 2024” programme, and from INFN through the project “BELL”. L.G. acknowledges support from the PNRR MUR project PE0000023-NQSTI, “National Quantum Science and Technology Institute”. G.A.F. acknowledges support from the ICSC – CentroNazionale di Ricerca in High-Performance Computing, Big Data and Quantum Computing. L.G. and G.A.F. acknowledge support from the University of Catania, Piano Incentivi Ricerca di Ateneo 2024-26, project TCMQI.

---

[1] G. Benenti, G. Casati, D. Rossini, and G. Strini, *Principles of Quantum Computation and Information*, 2nd ed.

(World Scientific, Singapore, 2018).

[2] A. Acín, I. Bloch, H. Buhrman, T. Calarco, C. Eichler, J. Eisert, D. Esteve, N. Gisin, S. J. Glaser, F. Jelezko, S. Kuhr, M. Lewenstein, M. F. Riedel, P. O. Schmidt, R. Thew, A. Wallraff, I. Walmsley, and F. K. Wilhelm, The quantum technologies roadmap: a European community view, *New Journal of Physics* **20**, 080201 (2018).

[3] A. Laucht, F. Hohls, N. Ubbelohde, M. Fernando Gonzalez-Zalba, D. J. Reilly, S. Stobbe, T. Schröder, P. Scarlino, J. V. Koski, A. Dzurak, C.-H. Yang, J. Yoneda, F. Kuemmeth, H. Bluhm, J. Pla, C. Hill, J. Salfi, A. Oiwa, J. T. Muhonen, E. Verhagen, M. D. LaHaye, H. H. Kim, A. W. Tsien, D. Culcer, A. Geresdi, J. A. Mol, V. Mohan, P. K. Jain, and J. Baugh, Roadmap on quantum nanotechnologies, *Nanotechnology* **32**, 162003 (2021).

[4] S. Campbell, I. D'Amico, M. A. Ciampini, J. Anders, N. Ares, S. Artini, A. Auffèves, L. B. Oftelie, L. P. Bettmann, M. V. Bonança, T. Busch, M. Campisi, M. F. Cavalcante, L. A. Correa, E. Cuestas, C. B. Dag, S. Dago, S. Deffner, A. del Campo, A. Deutschmann-Olek, S. Donadi, E. Doucet, C. Elouard, K. Ensslin, P. Erker, N. Fabbri, F. Fedele, G. Fiusa, T. Fogarty, J. A. Folk, G. Guarneri, A. S. Hegde, S. Hernández-Gómez, C.-K. Hu, F. Iemini, B. Karimi, N. Kiesel, G. Landi, A. Lasek, S. Lemziakov, G. Lo Monaco, E. Lutz, D. Lvov, O. Maillet, M. Mehboudi, T. M. Mendonça, H. J. D. Miller, A. K. Mitchell, M. Mitchison, V. Mukherjee, M. Paternostro, J. P. Pekola, M. Perarnau-Llobet, U. G. Poschinger, A. Rolandi, D. Rosa, R. Sánchez, A. C. Santos, R. S. Sarthour, E. Sela, A. Solfanelli, A. M. Souza, J. Splettstoesser, D. Tan, L. Tesser, T. V. Vu, A. Widera, N. Yunger Halpern, and K. Zawadzki, Roadmap on quantum thermodynamics, *Quantum Science and Technology* (2025).

[5] R. Alicki and M. Fannes, Entanglement boost for extractable work from ensembles of quantum batteries, *Phys. Rev. E* **87**, 042123 (2013).

[6] F. Campaioli, S. Gherardini, J. Q. Quach, M. Polini, and G. M. Andolina, Colloquium: Quantum batteries, *Rev. Mod. Phys.* **96**, 031001 (2024).

[7] D. Ferraro, F. Cavaliere, M. G. Genoni, G. Benenti, and M. Sassetto, Opportunities and challenges of quantum batteries, *Nature Reviews Physics* **10.1038/s42254-025-00906-5** (2026).

[8] F. Campaioli, F. A. Pollock, F. C. Binder, L. Céleri, J. Goold, S. Vinjanampathy, and K. Modi, Enhancing the charging power of quantum batteries, *Phys. Rev. Lett.* **118**, 150601 (2017).

[9] D. Ferraro, M. Campisi, G. M. Andolina, V. Pellegrini, and M. Polini, High-power collective charging of a solid-state quantum battery, *Phys. Rev. Lett.* **120**, 117702 (2018).

[10] S. Julià-Farré, T. Salamon, A. Riera, M. N. Bera, and M. Lewenstein, Bounds on the capacity and power of quantum batteries, *Phys. Rev. Res.* **2**, 023113 (2020).

[11] J.-Y. Gyhm, D. Šafránek, and D. Rosa, Quantum charging advantage cannot be extensive without global operations, *Phys. Rev. Lett.* **128**, 140501 (2022).

[12] D. Rinaldi, R. Filip, D. Gerace, and G. Guarneri, Reliable quantum advantage in quantum battery charging, *Phys. Rev. A* **112**, 012205 (2025).

[13] G. M. Andolina, V. Stanzione, V. Giovannetti, and M. Polini, Genuine quantum advantage in anharmonic bosonic quantum batteries, *Phys. Rev. Lett.* **134**, 240403 (2025).

[14] F. Cavaliere, D. Ferraro, M. Carrega, G. Benenti, and M. Sassetto, Quantum advantage bounds for a multiparticle gaussian battery (2025), [arXiv:2510.24162 \[quant-ph\]](https://arxiv.org/abs/2510.24162).

[15] J. Q. Quach, K. E. McGhee, L. Ganzer, D. M. Rouse, B. W. Lovett, E. M. Gauger, J. Keeling, G. Cerullo, D. G. Lidzey, and T. Virgili, Superabsorption in an organic microcavity: Toward a quantum battery, *Science Advances* **8**, eabk3160 (2022).

[16] K. Hymas, J. B. Muir, D. Tibben, J. van Embden, T. Hirai, C. J. Dunn, D. E. Gómez, J. A. Hutchison, T. A. Smith, and J. Q. Quach, Experimental demonstration of a scalable room-temperature quantum battery (2025), [arXiv:2501.16541 \[quant-ph\]](https://arxiv.org/abs/2501.16541).

[17] J. Joshi and T. S. Mahesh, Experimental investigation of a quantum battery using star-topology nmr spin systems, *Phys. Rev. A* **106**, 042601 (2022).

[18] C.-K. Hu, J. Qiu, P. J. P. Souza, J. Yuan, Y. Zhou, L. Zhang, J. Chu, X. Pan, L. Hu, J. Li, Y. Xu, Y. Zhong, S. Liu, F. Yan, D. Tan, R. Bachelard, C. J. Villas-Boas, A. C. Santos, and D. Yu, Optimal charging of a superconducting quantum battery, *Quantum Science and Technology* **7**, 045018 (2022).

[19] G. Gemme, M. Grossi, D. Ferraro, S. Vallecorsa, and M. Sassetto, Ibm quantum platforms: A quantum battery perspective, *Batteries* **8**, 43 (2022).

[20] G. Gemme, M. Grossi, S. Vallecorsa, M. Sassetto, and D. Ferraro, Qutrit quantum battery: Comparing different charging protocols, *Phys. Rev. Res.* **6**, 023091 (2024).

[21] L. Razzoli, G. Gemme, I. Khomchenko, M. Sassetto, H. Ouerdane, D. Ferraro, and G. Benenti, Cyclic solid-state quantum battery: thermodynamic characterization and quantum hardware simulation, *Quantum Science and Technology* **10**, 015064 (2025).

[22] S. Navid Elyasi, M. A. C. Rossi, and M. G. Genoni, Experimental simulation of daemonic work extraction in open quantum batteries on a digital quantum computer, *Quantum Science and Technology* **10**, 025017 (2025).

[23] C. Rodríguez, D. Rosa, and J. Olle, Artificial intelligence discovery of a charging protocol in a micromaser quantum battery, *Phys. Rev. A* **108**, 042618 (2023).

[24] P. A. Erdman, G. M. Andolina, V. Giovannetti, and F. Noé, Reinforcement learning optimization of the charging of a Dicke quantum battery, *Phys. Rev. Lett.* **133**, 243602 (2024).

[25] V. Evangelakos, E. Paspalakis, and D. Stefanatos, Fast charging of an Ising-spin-pair quantum battery using optimal control, *Phys. Rev. A* **110**, 052601 (2024).

[26] V. Evangelakos, E. Paspalakis, and D. Stefanatos, Rapid charging of a two-qubit quantum battery by transverse field amplitude and phase control, *Quantum Science and Technology* **10**, 035024 (2025).

[27] D. Meschede, H. Walther, and G. Müller, One-atom maser, *Phys. Rev. Lett.* **54**, 551 (1985).

[28] P. Filipowicz, J. Javanainen, and P. Meystre, Quantum and semiclassical steady states of a kicked cavity mode, *J. Opt. Soc. Am. B* **3**, 906 (1986).

[29] P. Meystre and M. Sargent, eds., *Elements of Quantum Optics*, 4th ed. (Springer Berlin Heidelberg, 2007).

[30] F. Ciccarello, S. Lorenzo, V. Giovannetti, and G. M. Palma, Quantum collision models: Open system dynamics from repeated interactions, *Physics Reports* **954**, 1 (2022).

[31] V. Shaghaghi, V. Singh, G. Benenti, and D. Rosa, Micromasers as quantum batteries, *Quantum Science and Technology* **7**, 04LT01 (2022).

[32] R. Salvia, M. Perarnau-Llobet, G. Haack, N. Brunner, and S. Nimmrichter, Quantum advantage in charging cavity and spin batteries by repeated interactions, *Phys. Rev. Res.* **5**, 013155 (2023).

[33] V. Shaghaghi, V. Singh, M. Carrega, D. Rosa, and G. Benenti, Lossy micromaser battery: Almost pure states in the Jaynes–Cummings regime, *Entropy* **25**, 430 (2023).

[34] N. Massa, F. Cavaliere, and D. Ferraro, The collisional charging of a transmon quantum battery, *Batteries* **11**, 240 (2025).

[35] C. Ciuti, G. Bastard, and I. Carusotto, Quantum vacuum properties of the intersubband cavity polariton field, *Phys. Rev. B* **72**, 115303 (2005).

[36] A. A. Anappara, S. De Liberato, A. Tredicucci, C. Ciuti, G. Biasiol, L. Sorba, and F. Beltram, Signatures of the ultrastrong light-matter coupling regime, *Phys. Rev. B* **79**, 201303 (2009).

[37] P. Forn-Díaz, J. Lisenfeld, D. Marcos, J. J. García-Ripoll, E. Solano, C. J. P. M. Harmans, and J. E. Mooij, Observation of the Bloch–Siegert shift in a qubit–oscillator system in the ultrastrong coupling regime, *Phys. Rev. Lett.* **105**, 237001 (2010).

[38] T. Niemczyk, F. Deppe, H. Huebl, E. P. Menzel, F. Hocke, M. J. Schwarz, J. J. García-Ripoll, D. Zueco, T. Hümmer, E. Solano, A. Marx, and R. Gross, Circuit quantum electrodynamics in the ultrastrong-coupling regime, *Nature Physics* **6**, 772 (2010).

[39] A. Blais, A. L. Grimsmo, S. M. Girvin, and A. Wallraff, Circuit quantum electrodynamics, *Rev. Mod. Phys.* **93**, 025005 (2021).

[40] F. Yoshihara, T. Fuse, S. Ashhab, K. Kakuyanagi, S. Saito, and K. Semba, Superconducting qubit–oscillator circuit beyond the ultrastrong-coupling regime, *Nature Physics* **13**, 44 (2017).

[41] K. V. Hovhannyan, F. Barra, and A. Imparato, Charging assisted by thermalization, *Phys. Rev. Res.* **2**, 033413 (2020).

[42] A. Crescente, M. Carrega, M. Sassetti, and D. Ferraro, Ultrafast charging in a two-photon dicke quantum battery, *Phys. Rev. B* **102**, 245407 (2020).

[43] F.-Q. Dou, Y.-Q. Lu, Y.-J. Wang, and J.-A. Sun, Extended dicke quantum battery with interatomic interactions and driving field, *Phys. Rev. B* **105**, 115405 (2022).

[44] A. Crescente, D. Ferraro, and M. Sassetti, Boosting energy transfer between quantum devices through spectrum engineering in the dissipative ultrastrong coupling regime, *Phys. Rev. Res.* **6**, 023092 (2024).

[45] F. Cavaliere, G. Gemme, G. Benenti, D. Ferraro, and M. Sassetti, Dynamical blockade of a reservoir for optimal performances of a quantum battery, *Communications Physics* **8**, 76 (2025).

[46] D. Manzano, A short introduction to the Lindblad master equation, *AIP Advances* **10**, 025106 (2020).

[47] F. Campaioli, J. H. Cole, and H. Hapuarachchi, Quantum master equations: Tips and tricks for quantum optics, quantum computing, and beyond, *PRX Quantum* **5**, 020202 (2024).

[48] H.-P. Breuer and F. Petruccione, *The Theory of Open Quantum Systems* (Oxford University Press, 2007).

[49] B. Vacchini, *Open Quantum Systems: Foundations and Theory*, 1st ed., Graduate Texts in Physics (Springer, Cham, 2024).

[50] C. P. Koch, U. Boscain, T. Calarco, G. Dirr, S. Filipp, S. J. Glaser, R. Kosloff, S. Montangero, T. Schulte-Herbrüggen, D. Sugny, and F. K. Wilhelm, Quantum optimal control in quantum technologies. Strategic report on current status, visions and goals for research in Europe, *EPJ Quantum Technology* **9**, 19 (2022).

[51] S. Haroche and J.-M. Raimond, *Exploring the Quantum: Atoms, Cavities, and Photons* (Oxford University Press, 2006).

[52] D. Braak, Integrability of the Rabi model, *Phys. Rev. Lett.* **107**, 100401 (2011).

[53] L. Razzoli, M. Crotti, and G. Benenti (2026), manuscript in preparation.

[54] A. Frisk Kockum, A. Miranowicz, S. De Liberato, S. Savasta, and F. Nori, Ultrastrong coupling between light and matter, *Nature Reviews Physics* **1**, 19 (2019).

[55] A. E. Allahverdyan, R. Balian, and T. M. Nieuwenhuizen, Maximal work extraction from finite quantum systems, *Europhysics Letters* **67**, 565 (2004).

[56] D. Rossini, G. M. Andolina, and M. Polini, Many-body localized quantum batteries, *Phys. Rev. B* **100**, 115142 (2019).

[57] W. Pusz and S. L. Woronowicz, Passive states and KMS states for general quantum systems, *Communications in Mathematical Physics* **58**, 273 (1978).

[58] A. Lenard, Thermodynamical proof of the Gibbs formula for elementary quantum systems, *Journal of Statistical Physics* **19**, 575 (1978).

[59] A. Kossakowski, On quantum statistical mechanics of non-Hamiltonian systems, *Reports on Mathematical Physics* **3**, 247 (1972).

[60] G. Lindblad, On the generators of quantum dynamical semigroups, *Communications in Mathematical Physics* **48**, 119 (1976).

[61] V. Gorini, A. Kossakowski, and E. C. G. Sudarshan, Completely positive dynamical semigroups of  $N$ -level systems, *Journal of Mathematical Physics* **17**, 821 (1976).

[62] T. Albash, S. Boixo, D. A. Lidar, and P. Zanardi, Quantum adiabatic Markovian master equations, *New Journal of Physics* **14**, 123016 (2012).

[63] G. Cenedese, S. T. Mister, M. Antezza, G. Benenti, and G. De Chiara, Thermodynamics and protection of discrete time crystals, *Phys. Rev. B* **112**, 054303 (2025).

[64] J. R. Johansson, P. D. Nation, and F. Nori, QuTiP: An open-source Python framework for the dynamics of open quantum systems, *Computer Physics Communications* **183**, 1760 (2012).

[65] J. R. Johansson, P. D. Nation, and F. Nori, QuTiP 2: A Python framework for the dynamics of open quantum systems, *Computer Physics Communications* **184**, 1234 (2013).

[66] P. Virtanen, R. Gommers, T. E. Oliphant, M. Haberland, T. Reddy, D. Cournapeau, E. Burovski, P. Peterson, W. Weckesser, J. Bright, S. J. van der Walt, M. Brett, J. Wilson, K. J. Millman, N. Mayorov, A. R. J. Nelson, E. Jones, R. Kern, E. Larson, C. J. Carey, I. Polat, Y. Feng, E. W. Moore, J. VanderPlas, D. Laxalde, J. Perktold, R. Cimrman, I. Henriksen, E. A. Quintero, C. R. Harris, A. M. Archibald, A. H. Ribeiro, F. Pedregosa, P. van Mulbregt, and the SciPy 1.0 Contributors, Scipy 1.0: Fundamental algorithms for scientific computing in python, *Nature Methods* **17**, 261 (2020).

[67] F. Beaudoin, J. M. Gambetta, and A. Blais, Dissipation

and ultrastrong coupling in circuit QED, *Phys. Rev. A* **84**, 043832 (2011).

[68] J. M. Fink, M. Göppl, M. Baur, R. Bianchetti, P. J. Leek, A. Blais, and A. Wallraff, Climbing the Jaynes-Cummings ladder and observing its nonlinearity in a cavity QED system, *Nature* **454**, 315 (2008).

[69] A. L. Grimsmo and S. Parkins, Cavity-QED simulation of qubit-oscillator dynamics in the ultrastrong-coupling regime, *Phys. Rev. A* **87**, 033814 (2013).

[70] F. Mazzoncini, V. Cavina, G. M. Andolina, P. A. Erdman, and V. Giovannetti, Optimal control methods for quantum batteries, *Phys. Rev. A* **107**, 032218 (2023).

[71] J. C. López Carreño, Wigner function of observed quantum systems, *New Journal of Physics* **27**, 043009 (2025).

[72] W. B. Case, Wigner functions and weyl transforms for pedestrians, *American Journal of Physics* **76**, 937 (2008).

[73] H. M. Wiseman and G. J. Milburn, *Quantum Measurement and Control* (Cambridge University Press, 2009).

[74] F. Albarelli and M. G. Genoni, A pedagogical introduction to continuously monitored quantum systems and measurement-based feedback, *Physics Letters A* **494**, 129260 (2024).

[75] M. T. Mitchison, J. Goold, and J. Prior, Charging a quantum battery with linear feedback control, *Quantum* **5**, 500 (2021).

[76] Y. Yao and X. Q. Shao, Optimal charging of open spin-chain quantum batteries via homodyne-based feedback control, *Phys. Rev. E* **106**, 014138 (2022).

[77] A. de Oliveira Junior, J. B. Brask, and R. Chaves, A friendly guide to exorcising Maxwell's demon, *PRX Quantum* **6**, 030201 (2025).

[78] G. Francica, J. Goold, F. Plastina, and M. Paternostro, Daemonic ergotropy: Enhanced work extraction from quantum correlations, *npj Quantum Information* **3**, 12 (2017).

[79] G. Manzano, F. Plastina, and R. Zambrini, Optimal work extraction and thermodynamics of quantum measurements and correlations, *Phys. Rev. Lett.* **121**, 120602 (2018).

[80] D. Morrone, M. A. Rossi, and M. G. Genoni, Daemonic ergotropy in continuously monitored open quantum batteries, *Phys. Rev. Appl.* **20**, 044073 (2023).

[81] G. Cenedese, G. Benenti, D. Ferraro, and M. G. Genoni, Boosting work extraction in quantum batteries via continuous environment monitoring (2025), arXiv:2512.05244 [quant-ph].